

REPORT DOCUMENTATION PAGE

Form Approved
OMB No. 0704-0188

Public reporting burden for this collection of information is estimated to average 1 hour per response, including the time for reviewing instructions, searching existing data sources, gathering and maintaining the data needed, and completing and reviewing this collection of information. Send comments regarding this burden estimate or any other aspect of this collection of information, including suggestions for reducing this burden to Department of Defense, Washington Headquarters Services, Directorate for Information Operations and Reports (0704-0188), 1215 Jefferson Davis Highway, Suite 1204, Arlington, VA 22202-4302. Respondents should be aware that notwithstanding any other provision of law, no person shall be subject to any penalty for failing to comply with a collection of information if it does not display a currently valid OMB control number. PLEASE DO NOT RETURN YOUR FORM TO THE ABOVE ADDRESS.

1. REPORT DATE (DD-MM-YYYY) 05-12-2005		2. REPORT TYPE REPRINT		3. DATES COVERED (From - To)	
4. TITLE AND SUBTITLE A PULSED-FIELD IONIZATION PHOTOELECTRON SECONDARY ION COINCIDENCE STUDY OF THE $H^+(X, v^+ = 0 - 15, N^+ = 1) + He$ PROTON TRANSFER REACTION ²				5a. CONTRACT NUMBER	
				5b. GRANT NUMBER	
				5c. PROGRAM ELEMENT NUMBER 61102F	
6. AUTHOR(S) X. N. Tang*, H. Xu*, T. Zhang*, Y. Hou*, C. Chang*, C.Y. Ng* Y. Chiu, R.A. Dressler, and D. J. Levandier**				5d. PROJECT NUMBER 2303	
				5e. TASK NUMBER RS	
				5f. WORK UNIT NUMBER A1	
7. PERFORMING ORGANIZATION NAME(S) AND ADDRESS(ES) Air Force Research Laboratory/VSBXT 29 Randolph Road Hanscom AFB MA 01731-3010				8. PERFORMING ORGANIZATION REPORT NUMBER AFRL-VS-HA-TR-2005-1170	
9. SPONSORING / MONITORING AGENCY NAME(S) AND ADDRESS(ES)				10. SPONSOR/MONITOR'S ACRONYM(S)	
				11. SPONSOR/MONITOR'S REPORT NUMBER(S)	
12. DISTRIBUTION / AVAILABILITY STATEMENT Approved for Public Release; Distribution Unlimited *Dept. Chemistry, Univ Calif Davis, CA; **Boston College, Institute for Sci Res., Newton, MA					
13. SUPPLEMENTARY NOTES REPRINTED FROM: THE JOURNAL OF CHEMICAL PHYSICS, Vol 122, 164301 (2005).					
14. ABSTRACT The endothermic proton transfer reaction, $H_2^+(v^+) + He \rightarrow HeH^+ + H (\Delta E = 0.806 \text{ eV})$, is investigated over a broad range of reactant vibrational levels using high-resolution vacuum ultraviolet to prepare reactant ions either through excitation of autoionization resonances, or using the pulsed-field ionization-photoelectron-secondary ion coincidence (PFI-PESICO) approach. In the former case, the translational energy dependence of the integral reaction cross sections are measured for $v^+ = 0-3$ with high signal-to-noise using the guided-ion beam technique. PFI-PESICO cross sections are reported for $v^+ = 1-15$ and $v^+ = 0-12$ at center-of-mass collision energies of 0.6 and 3.1 eV, respectively. All ion reactant states selected by the PFI-PESICO scheme are in the $N^+ = 1$ rotational level. The experimental cross sections are complemented with quasiclassical trajectory (QCT) calculations performed on the <i>ab initio</i> potential energy surface provided by Palmieri <i>et al.</i> [Mol. Phys. 98, 1839 (2000)]. The QCT cross sections are significantly lower than the experimental results near threshold, consistent with important contributions due to resonances observed in quantum scattering studies. At total energies above 2 eV, the QCT calculations are in excellent agreement with the present results. PFI-PESICO time-of-flight (TOF) measurements are also reported for $v^+ = 3$ and 4 at a collision energy of 0.6 eV. The velocity inverted TOF spectra are consistent with the prevalence of a spectator-stripping mechanism.					
15. SUBJECT TERMS Pulsed-field ionization Coincidence measurements Proton transfer State-selected reaction dynamics Vibrational state selection Synchrotron radiation					
16. SECURITY CLASSIFICATION OF:			17. LIMITATION OF ABSTRACT SAR	18. NUMBER OF PAGES	19a. NAME OF RESPONSIBLE PERSON R. Dressler
a. REPORT UNCLAS	b. ABSTRACT UNCLAS	c. THIS PAGE UNCLAS			19b. TELEPHONE NUMBER (include area code) 781-377-2332

A pulsed-field ionization photoelectron secondary ion coincidence study of the $\text{H}_2^+(X, v^+=0-15, N^+=1) + \text{He}$ proton transfer reaction

X. N. Tang, H. Xu, T. Zhang, Y. Hou, C. Chang, and C. Y. Ng^{a)}
Department of Chemistry, University of California at Davis, Davis, California 95616

Y. Chiu and R. A. Dressler^{b)}
Air Force Research Laboratory, Space Vehicles Directorate, Hanscom Air Force Base, Massachusetts 01731-3010

D. J. Levandier
Boston College, Institute for Scientific Research, Newton, Massachusetts 02159

(Received 5 January 2005; accepted 7 February 2005; published online 22 April 2005)

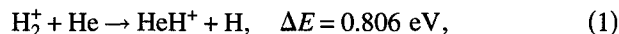
The endothermic proton transfer reaction, $\text{H}_2^+(v^+) + \text{He} \rightarrow \text{HeH}^+ + \text{H} (\Delta E = 0.806 \text{ eV})$, is investigated over a broad range of reactant vibrational levels using high-resolution vacuum ultraviolet to prepare reactant ions either through excitation of autoionization resonances, or using the pulsed-field ionization-photoelectron-secondary ion coincidence (PFI-PESICO) approach. In the former case, the translational energy dependence of the integral reaction cross sections are measured for $v^+ = 0-3$ with high signal-to-noise using the guided-ion beam technique. PFI-PESICO cross sections are reported for $v^+ = 1-15$ and $v^+ = 0-12$ at center-of-mass collision energies of 0.6 and 3.1 eV, respectively. All ion reactant states selected by the PFI-PESICO scheme are in the $N^+ = 1$ rotational level. The experimental cross sections are complemented with quasiclassical trajectory (QCT) calculations performed on the *ab initio* potential energy surface provided by Palmieri *et al.* [Mol. Phys. **98**, 1839 (2000)]. The QCT cross sections are significantly lower than the experimental results near threshold, consistent with important contributions due to resonances observed in quantum scattering studies. At total energies above 2 eV, the QCT calculations are in excellent agreement with the present results. PFI-PESICO time-of-flight (TOF) measurements are also reported for $v^+ = 3$ and 4 at a collision energy of 0.6 eV. The velocity inverted TOF spectra are consistent with the prevalence of a spectator-stripping mechanism. © 2005 American Institute of Physics. [DOI: 10.1063/1.1883169]

I. INTRODUCTION

Recently, we have demonstrated that the pulsed-field ionization photoelectron secondary ion coincidence (PFI-PESICO) approach using quasicontinuous synchrotron radiation^{1,2} provides the sensitivity to investigate the state-selected reactivity of H_2^+ ions over a broad vibrational energy range including states approaching the dissociation limit.³ In our investigation of the $\text{H}_2^+ + \text{Ne}$ proton transfer system³ we succeeded in measuring an absolute integral reaction cross section for H_2^+ populated in the $v^+ = 17, N^+ = 1$ rovibrational level which lies merely 0.03 eV below the dissociation limit. Quasiclassical trajectory (QCT) calculations were found to be in good agreement with the observed state-selected cross sections at intermediate total energies (1–3 eV). Discrepancies at low total energies were attributed to resonances, which had been observed in numerous quantum scattering studies,^{4–7} while at high energies, it was suggested that possibly nonadiabatic effects, or inaccuracies in the applied potential,⁸ could explain that QCT appeared to overpredict the competitive effect of the collision-induced dissociation (CID) channel. Significant discrepancies exist between the

measured cross sections and those of a number of quantum-scattering studies that used the same potential energy surface.^{5–7} The calculated cross sections for $v^+ > 0$ at low total energies ($E < 1$ eV) were significantly higher than the measured values, suggesting a possible overemphasis of resonances in the theoretical work which again may be attributed to an inaccurate potential.

The prototype three-electron $\text{H}_2^+ + \text{He}$ proton transfer system,



has been an important test case for theoretical methods of reaction dynamics for the past 30 years. Consequently, a substantially more extended body of theoretical work exists for this reaction. As in the $\text{H}_2^+ + \text{Ne}$ case, Chupka and co-workers^{9–11} discovered in the first state-selected ion-molecule reaction studies that this endothermic reaction is promoted much more effectively by vibrational energy than translational energy. Except for one early quantum mechanical¹² and QCT study,¹³ reaction probabilities determined in collinear geometry quantum^{14–16} and QCT reactive scattering studies^{17,18} do not reflect the experimentally observed vibrational enhancement in the integral reaction cross sections. The first theoretical confirmation of the large vibrational effects was obtained by Whitton and Kuntz,^{19,20} who

^{a)}Electronic mail: cyng@chem.ucdavis.edu

^{b)}Electronic mail: rainer.dressler@hanscom.af.mil

conducted three-dimensional (3D) QCT calculations based on an approximate diatomics-in-molecules potential fit²¹ to *ab initio* points of collinear H_2He^+ by Brown and Hayes.²² Additional 3D QCT studies^{23–25} and a quantum-mechanical reactive scattering study using the infinite-order sudden approximation (RIOSA)²⁶ based on various fits to the Hayes and Brown *ab initio* points were consistent with the experimental results from Chupka *et al.* that show that vibrational energy enhances the reaction more effectively than translational energy.

A significantly improved potential energy surface was obtained from a fit by Joseph and Sathyamurthy^{27,28} to a new set of *ab initio* points including noncollinear geometries that were calculated with configuration interaction accuracy by McLaughlin and Thompson.²⁹ 3D QCT calculations²⁸ on this surface, which is generally referred to as MTJS, were in satisfactory agreement with the Chupka measurements.^{9–11} However, the accuracy of QCT calculations, even on an exact potential energy surface, is put into question with the observation of highly oscillatory behavior attributed to resonances in the energy spectrum of inelastic^{30,31} and reactive^{14,15,32–38} scattering probabilities in collinear quantum-mechanical studies. The new 3D MTJS surface spawned a series of 3D quantum scattering studies providing reaction probabilities for zero total angular momentum ($J=0$)^{37,39–44} as well as integral cross sections ($J\neq 0$)^{39,41,45} all of which confirm dense resonance structure. The importance of resonances, which have been associated with a well in the entrance channel, makes an accurate 3D potential energy surface a prerequisite to reliable cross-section calculations at low total energies. Improved fitting algorithms⁴⁶ and new, more extended and higher-level sets of *ab initio* points^{47,48} have led to more precise surfaces^{47–50} with more accurate dispersion-force description at long range.⁴⁹ Kumar *et al.*⁵¹ found large differences in QCT integral cross-section calculations depending on whether the MTJS surface or the more sophisticated Aguado–Paniagua⁴⁶ fit to the same McLaughlin–Thompson *ab initio* points is applied.

Despite the extensive theoretical work, relatively few opportunities to compare the computational results to experimental data exist. In particular, absolute cross-section measurements for well-characterized internal and translational energies are rather scarce. Given the high endothermicity, thermal experiments that relax the H_2^+ internal energy are not possible, while electron-impact ionization approaches without efficient reactant relaxation produce the reactant ions in a broad distribution of vibrational levels resulting in rate coefficients that are averaged over the precursor population.^{52,53} Van Pijkeren *et al.* determined relative state-selected cross sections up to $v^+=8$ at thermal energies using a coincidence technique.^{54,55} The original state-selected work by Chupka and co-workers^{9–11} did not directly determine absolute cross sections, and the experimental arrangement did not have good control over the translational energy. Nevertheless, they were able to convert their phenomenological cross sections to microscopic state-selected cross sections¹⁰ using an approach outlined by Light.⁵⁶ The respective absolute cross sections have since been propagated through the literature. Turner *et al.*⁵⁷ used the guided-ion beam (GIB) technique

and vacuum ultraviolet (VUV) direct ionization to derive absolute state-selected cross sections for H_2^+ and HD^+ , $v^+=0–4$ in a well-defined translational energy range of 1–8 eV. The analysis required knowledge of the H_2^+ vibrational distribution at the selected VUV ionizing wavelengths, which had a significantly higher photon bandwidth of 4 Å in comparison to the Chupka experiments (0.4–2.5 Å). Beam studies with pure state selection, using the threshold electron secondary ion coincidence technique, were carried out by Koyano and co-workers,^{26,58} who reported relative cross sections for $v^+=0–4$ at translational energies ranging from 0.4 to 3.0 eV. Govers and Guyon also applied a coincidence technique to measure relative cross sections for $v^+=0–6$ at a center-of-mass (c.m.) collision energy of 3.1 eV. Absolute cross sections were obtained by scaling them to the cross sections reported by Chupka.^{9–11} Achtenhagen, Schweizer, and Gerlich,⁵⁹ in unpublished results first reported by Kumar *et al.*,⁶⁰ measured the translational energy dependence of absolute cross sections for $\text{H}_2^+(v^+=0, 1)$ prepared by 3+1 resonance enhanced multiphoton ionization. It is known that the vibrational state selection is somewhat affected by contamination in this approach.⁶¹

Additional opportunities for comparison between experiment and theory have been provided by angular distribution measurements carried out in crossed-beam experiments, where both unrelaxed^{62,63} and relaxed^{58,64} electron-impact ionization sources, and state-selected ions using a multiphoton ionization technique^{65,66} have been used. Probably the most sensitive test of theoretical methods to date has been the comparison between theoretical^{43,67} and experimental branching ratios in HD^+ reactions with He, where Turner *et al.* have produced the only experimental data.⁵⁷

In the present paper, we apply the PFI-PESICO technique to this fundamental chemical reaction. Absolute cross sections are reported for significantly higher vibrational levels than previous measurements at translational energies of 0.6 and 3.1 eV. Given the extended theoretical work at low total energies, we also present the translational energy dependence of cross sections for the first four vibrational levels of H_2^+ for which the present experiment has very high sensitivity due to intense VUV absorption resonances associated with Rydberg states that are known to preferably autoionize to the next lowest ionic level. We complement the cross-section measurements with samples of recoil velocity distribution measurements as well as with QCT calculations performed on the recent 3D potential energy surface reported by Palmieri, Aquilanti, and co-workers.^{47,48}

II. EXPERIMENT

The PFI-PESICO experiment as applied to H_2^+ reactions, and the associated signal processing has been described in detail previously.^{1–3} A brief description with particular emphasis on modifications of the instrument will be provided here. An effusive beam of H_2 is ionized with monochromatic VUV synchrotron radiation generated at the Chemical Dynamics Beamline Endstation 2 of the ALS. The VUV is passed through a high-resolution 6.65 m monochromator providing a resolution between 2 and 10 cm^{-1} . In the PFI-

PESICO experiments, the VUV is tuned to excite H_2 molecules to high- n Rydberg states below the ionization limit of an ionic quantum state of interest. A pulsed ionization and extraction electric field (~ 8 V/cm, 200 ns duration) is applied approximately 10 ns after the onset of the 104 ns dark gap of the multibunch operation mode of the storage ring.^{68,69} Long-lived Rydberg molecules in the photoionization region are field ionized and accelerated toward the injection electrode of a guided-ion beam (GIB) experiment. The correlated PFI-electrons are accelerated in the opposite direction toward a time-of-flight (TOF) electron spectrometer equipped with a microchannel plate detector.

A fast interleaved comb wire gate^{70,71} is situated between the GIB injection electrode and the photoionization region. The gate is opened for ~ 250 ns to transmit ions at a fixed delay with respect to the detection of a PFI electron. This allows the transmission of the associated PFI ion, while rejecting false coincidences due to prompt photoions during the closed state. The gate is opened a second time some 200 μ s after the first gate in order to provide a measure of the false coincidence signal level.

The ion guide consists of tandem rf-octopoles (8.64 and 19.55 cm long, 2 mm rod diameter on 8 mm diameter circle, 13 MHz rf frequency), where the first octopole guides the ion beam through a collision cell containing ~ 0.2 mTorr of He target gas. Primary and secondary ions enter the second longer octopole which is biased approximately 0.4 eV lower than the first in order to accelerate near-thermal ions to prevent losses due to surface potential barriers. Ions are extracted from the second octopole and injected into a quadrupole mass filter following which they are detected with a Daly detector.⁷² Primary and secondary ions are recorded on a multichannel scaler in a time-resolved way. Integral cross sections are determined from the expression

$$\sigma_i = \frac{I_i}{(\sum_j I_j + I_p)nl}, \quad (2)$$

where I_p is the primary ion count rate, I_j are the secondary ion intensities, n is the target gas density, and l is the effective path length of the collision cell. The ion count rates are corrected for false-coincidences appearing during the second gate opening period, at long delays in the time-resolved ion recordings.

Cross sections are also measured in an automated collision-energy scanning approach for those H_2^+ vibrational levels that can be prepared with high purity by selectively exciting autoionizing resonances with known decay branching ratios.^{73,74} The ion laboratory energy resolution is determined to be 0.3 eV [Full width at half maximum (FWHM)] for this mode using retardation and TOF methods.³ In the PFI-PESICO mode, the resolution is estimated to be around 0.3 eV as well from TOF analysis.³ The c.m. collision energy resolution is increasingly affected by the motion of the target gas as the collision energy is raised, as described by Chantry.⁷⁵ At $E_T=0.6$ eV, the c.m. collision energy resolution is ~ 0.3 eV (FWHM), whereas at 3.1 eV, the second energy at which we have performed PFI-PESICO experiments, it has increased to 0.58 eV.

In comparison to our earlier H_2^++Ne measurements, the position of the center of mass of the H_2^+He collision system is more favorable to allow an analysis of recoil velocity distributions based on the PFI-PESICO TOF measurements. For this purpose, the PFI-PESICO TOF measurements are inverted to velocity distributions following subtraction of the false coincidence spectrum. The methodology for this transformation has been described earlier.⁷⁶

III. COMPUTATION

The QCT calculations were performed using a modified version³ of the $A+BC$ QCT program by Chapman *et al.*⁷⁷ based on the theory of Truhlar and Muckerman.⁷⁸ Trajectories were calculated on the V_{12}^1 potential provided by Palmieri *et al.*⁴⁷ that was obtained by fitting the functional form given by Aguado and Paniagua⁴⁶ to *ab initio* points calculated for 1487 different geometries. With this surface, the total energy is conserved to within 0.01% for all initial conditions presented, here. Between 3000 and 5000 trajectories are calculated for each reported cross section. Given the important differences in classical and quantum mechanical threshold energies, two QCT results are considered. In a first purely classical result, all proton transfer channels associated with a translational energy transfer corresponding to bound product ions, HeH^+ , are taken into account when determining the cross section. In a second, proton transfer channels are disregarded for which the vibrational energy of HeH^+ is less than the zero point energy of 0.195 eV. Two approaches are also applied with respect to the collision-induced dissociation (CID) channel ($He+H^++H$). In the first, molecular products with internal energies exceeding the dissociation threshold are considered dissociated, and these trajectories contribute to the total CID channel count. In order to compare directly with our experimental results, such channels with quasibound molecular scattering products, H_2^+ and HeH^+ , were identified and the lifetime of the quasibound products were determined using the approach by Kuntz.⁷⁸ In the second approach, those trajectories with quasibound lifetimes exceeding the respective average instrumental flight times of H_2^+ and HeH^+ were added to the corresponding non-reactive and reactive total.

IV. RESULTS

A. Translational energy dependence of the $H_2^+(v^+=0, 1, 2, 3)+He$ proton transfer cross sections

Figure 1(a) shows photoionization efficiency (PIE) curves for reactant H_2^+ ions in the VUV energy range of 15.40–16.45 eV obtained using an optical bandwidth of 8 cm^{-1} . The ionization thresholds associated with the formation of the $H_2^+(v^+=0, 1, 2, 3, \text{ and } 4)$ vibrational levels at 15.4252, 15.69767, 15.9541, 16.1939, and 16.4202 eV, respectively, are marked at the top of Fig. 1(a). The PIE spectrum for H_2 is dominated by strong autoionization features with only minor continuum components contributed by direct photoionization. The autoionization resonances have been analyzed in detail in the high resolution measurements by Dehmer and Chupka.⁷³ Due to the propensity for vibra-

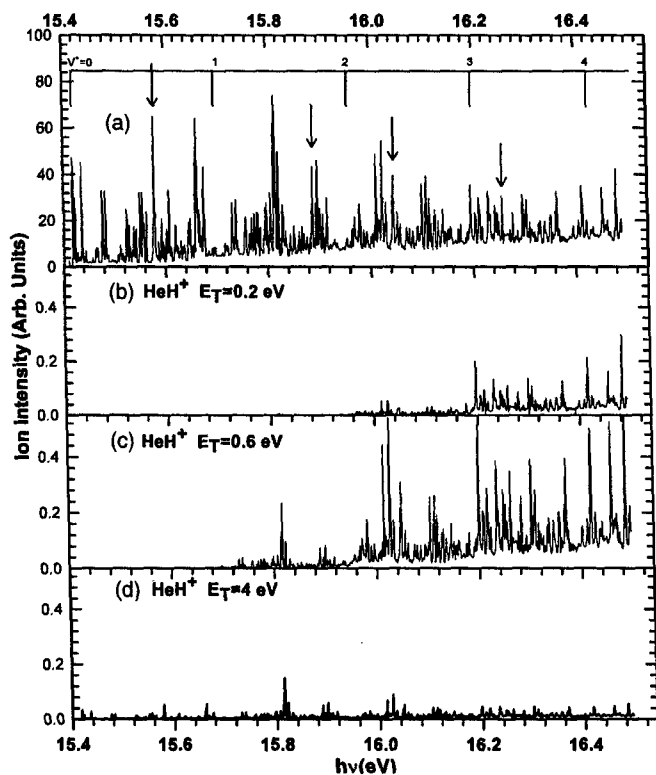


FIG. 1. Photoionization efficiency curves for primary and proton-transfer secondary ions transmitted through the guided-ion beam apparatus when He is introduced into the collision cell. Secondary ion curves are shown for different center-of-mass collision energies, E_T . Arrows indicate the photon energies at which proton-transfer cross-section energy scans, shown in Fig. 2, were recorded.

tional autoionization, autoionizing peaks of H_2 resolved in the vibrational interval of v^+ and v^++1 are shown to produce reactants predominantly in the $H_2^+(v^+)$ level.

The PIE spectra for the formation of proton transfer product HeH^+ ions, as transmitted through the GIB apparatus at the center-of-mass collision energies, E_T , of 0.2, 0.6, and 4.0 eV are depicted in Figs. 1(b)–1(d), respectively. We note that the ion intensity scales for Figs. 1(a)–1(d) have the same (arbitrary) units. Given the high vibrational energy dependence of the proton transfer reaction, the PIE curves for product HeH^+ provide a good assessment with respect to the decay branching ratios into ionic vibrational states of particular autoionization resonances. If the ratio of the intensity of two product ion autoionization lines, for which the branching ratio of one line has been determined, is equal to that of the same lines in the reactant ion PIE curve, it can be concluded that the reaction cross sections for ions prepared through photoionization via both resonances is the same, and thus the vibrational state selection purity is identical. The only branching ratios available are those measured by O'Halloran *et al.* in a narrow range of photon energies between the photoionization limits of $v^+=1$ and 2 .⁷⁴ Most of the vibrational branching ratios to $v^+=1$ in the investigated region between 14.885 and 14.927 eV are between 94% and 96%. We have verified that the ratio between the PIE intensities of the selected resonance and those investigated by O'Halloran are equal.

The $H_2^+(v^+)+He$ proton transfer reaction is a model sys-

tem for the demonstration of translational and vibrational energy effects on the reaction cross sections. Considering that the endothermicity for reaction (1) is 0.806 eV, which is greater than the internal energy of $H_2^+(v^+=3)$, 0.7683 eV, we expect that the proton transfer channel of $H_2^+(v^+\leq 3)+He$ is closed at $E_T < 0.037$ eV. At $E_T = 0.2$ eV, the proton transfer channel of $H_2^+(v^+=3)+He$ is open, as evidenced by the PIE step of HeH^+ at 16.19 eV, which corresponds to the photoionization threshold for forming $H_2^+(v^+=3)$, as observed in Fig. 1(b). The autoionization line intensities for HeH^+ associated with the formation of reactant $H_2^+(v^+=2)$ in the VUV region of 15.95–16.19 eV are found to be nonzero, but are significantly lower than those for the formation of $H_2^+(v^+=3)$. The finite intensities for HeH^+ arising from the $H_2^+(v^+=2)+He$ can be attributed to the uncertainty in E_T of ≈ 0.2 eV for the present measurements at low E_T . This arises from the fact that the proton transfer reactions of $H_2^+(v^+=2$ and $3)+He$ are promoted by translational energy near threshold.

Comparing the PIE curve for reactant H_2^+ of Fig. 1(a) and that for HeH^+ of Fig. 1(b), we can also conclude that the formation of HeH^+ is higher for the $H_2^+(v^+=4)+He$ compared to that of $H_2^+(v^+=3)+He$. As E_T is increased to 0.6 eV, the proton transfer reaction of $H_2^+(v^+=1)+He$ is energetically allowed, as observed in the PIE onset of HeH^+ in Fig. 1(c). The comparison of the PIE spectra for reactant H_2^+ of Fig. 1(a) and HeH^+ of Fig. 1(c) shows that the vibrational-state-selected integral proton transfer cross sections [$\sigma(v^+)$] at $E_T = 0.6$ eV are in the order: $\sigma(v^+=1) \ll \sigma(v^+=2) < \sigma(v^+=3)$. Figure 1(d) illustrates that at $E_T = 4$ eV, the proton transfer reaction occurs for all $H_2^+(v^+=0-4)$ states. However, the cross sections for the formation of HeH^+ at $E_T = 4$ eV are significantly lower than those at $E_T = 0.2$ and 0.6 eV.

The selected H_2 autoionization resonances for the translational energy scans of state-selected cross sections for $H_2^+(v^+=0, 1, 2, \text{ and } 3)$ are marked by downward pointing arrows in the upper panel of Fig. 1(a). Figure 2 compares the measured state-selected integral cross sections obtained when scanning the primary ion kinetic energy in the first octopole while maintaining the VUV ionizing radiation at photon energies identified in Table I to prepare the respective reactant vibrational states. The present experimental data in Fig. 2 were not corrected with respect to an assumed autoionization resonance decay branching ratio. The errors in absolute value of the measured cross sections are estimated at $\pm 30\%$. However, given the uncertainty in state purity, the cross sections for $v^+=2$ and 3 must be considered lower limits.

TABLE I. Experimental parameters associated with the measurements of Fig. 2. $h\nu$ is the photon energy used to excite specified autoionization resonances, and A , $E_0 - E_i$, and n are the modified LOC fit parameters determined from a nonlinear least-squares fit to the experimental data.

v^+	$h\nu$ (eV)	Resonance	A ($\text{\AA}^2 \text{eV}^{-(n-1)}$)	$E_0 - E_i$ (eV)	n
0	15.5779	$6p\pi, v=2$	0.143	0.783	0.77
1	15.8876	$5p\pi, v=4$	0.574	0.523	0.36
2	16.0450	$6p\pi, v=4$	1.36	0.248	0.44
3	16.2556	$6p\pi, v=5$	3.40	0.082	0.49

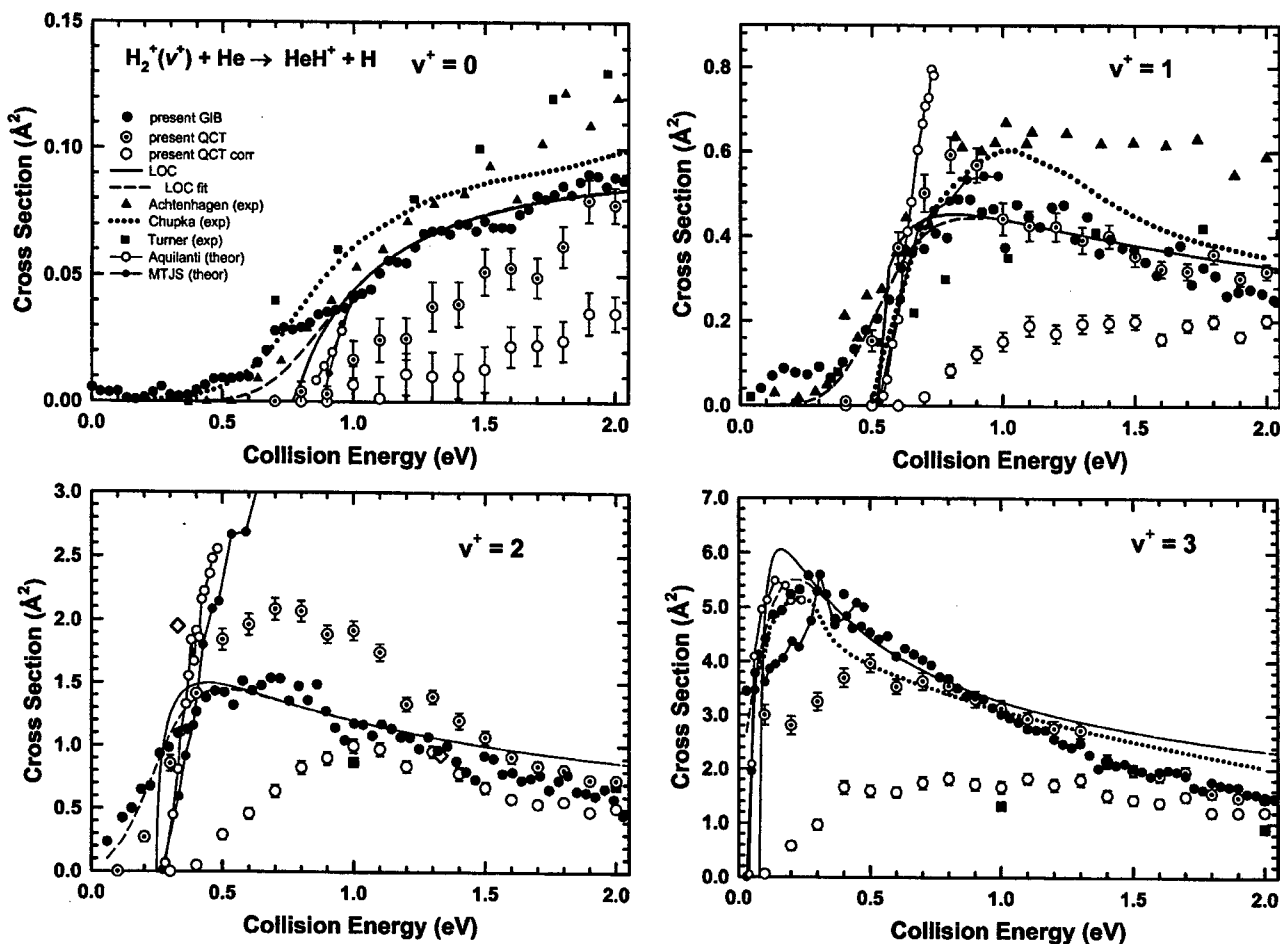


FIG. 2. The low-energy translational energy dependence of the $\text{H}_2^+ + \text{He}$ proton transfer cross section for primary ions state-selected in $v^+=0-3$ through autoionization (present GIB). The selected autoionization resonances are pointed out in Fig. 1 and listed in Table I. LOC designates the deconvoluted modified line-of-centers model [Eq. (3)] cross sections of the present GIB measurements. LOC fit is the corresponding fit to the experimental data including kinematic broadening. QCT and QCT corr are the present QCT calculations with and without zero-point energy corrections. Data labeled MTJS refer to quantum reactive scattering studies by Lepetit and Launay—Ref. 41 (only $v^+=0$) and time-dependent quantum scattering studies by Maiti *et al.*—Ref. 45 (all others). The present results are also compared with experimental work by Achtenhagen *et al.* (Ref. 59), Chupka and co-workers (Refs. 9–11), and Turner *et al.* (Ref. 57), and quantum theoretical calculations by Aquilanti *et al.* (Ref. 48).

The present measurements are compared with the measurements of Chupka *et al.*,^{9–11} and GIB measurements of Turner *et al.*⁵⁷ and Achtenhagen *et al.*⁵⁹ Note that the cross sections from Chupka *et al.* at $v^+=1$ were taken from the analysis of Kumar *et al.*^{60,79} and are not reported as such by the original authors. The experimental data are compared with presently calculated quasiclassical trajectories based on the surface reported by Palmieri *et al.*⁴⁷ The dotted circles are the pure classical results, while the open circles correspond to zero-point energy corrected values. A comparison with 3D quantum reactive scattering calculations of the threshold region using the MTJS surface by Lepetit and Launay⁴¹ ($v^+=0$) and Maiti *et al.*⁴⁵ (all other vibrational states, time dependent approach) and Aquilanti *et al.*⁴⁸ (surface determined by Palmieri *et al.*⁴⁷) is also provided. The quantum calculations determine a very sharp onset of the reaction cross section at threshold. Although such a sharp onset is not necessarily reproduced by the experiments, it must be emphasized that the energy resolution of the experiments is kinematically broadened by the ion beam energy resolution (~ 0.3 eV FWHM) and the thermal motion of the target gas. As in our previous study on the $\text{H}_2^+ + \text{Ne}$ system,³

we have attempted to deconvolute the present experimental cross sections using the modified line-of-centers (LOC) functional form,^{80,81}

$$\sigma = A \frac{(E_T + E_i - E_0)^n}{E_T}, \quad (3)$$

where E_T is the translational or collision energy, A is a scaling parameter, $E_0 = 0.806$ eV is the threshold energy, E_i is the internal energy, and n is the curvature parameter. A nonlinear least-squares fitting algorithm is used that takes all experimental broadening mechanisms into account. The dashed curves in Fig. 2 are the model fits. The deconvoluted cross sections, corresponding to Eq. (3) and the fit parameters listed for each reactant vibrational state in Table I, are given by the solid lines.

The deconvoluted cross sections provide sharp threshold behavior except for $v^+=0$. In the latter case, we fixed the threshold to a value corresponding to the 0 K thermochemical threshold energy with added thermal rotational energy since a free fit of the three parameters would have resulted in a threshold energy that was too low. Given the very small

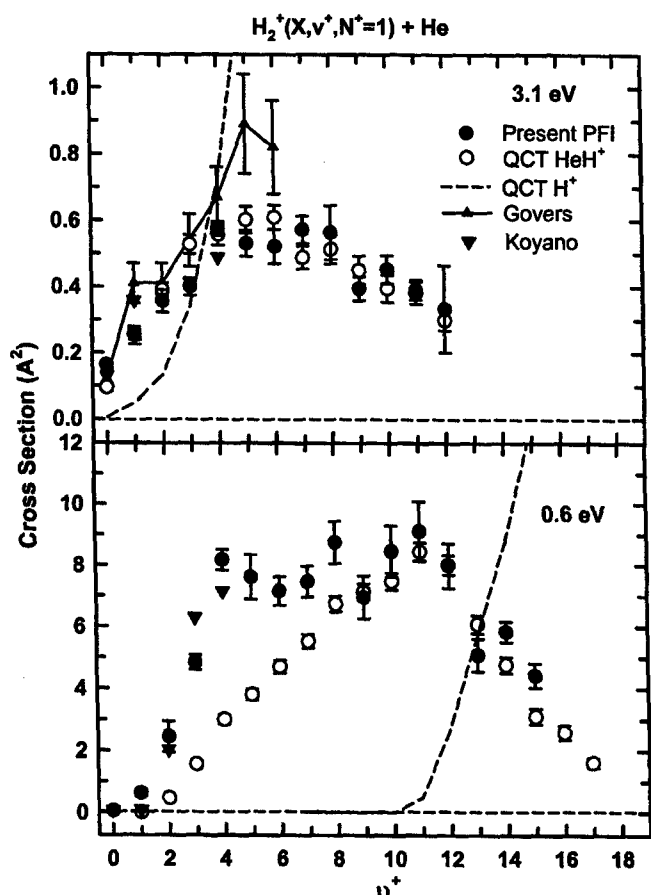


FIG. 3. PFI-PESICO cross sections (present PFI) as a function of reactant vibrational level at collision energies $E_T=0.6$ and 3.1 eV (c.m.). All reactants are prepared in the $N^+=1$ rotational state. The present experimental results are compared with present QCT proton transfer (QCT HeH $^+$) and CID (QCT H $^+$) cross sections, and experimental work by Govers and Guyon (Ref. 82) and Koyano and co-workers (Refs. 26 and 58). The QCT results are corrected with respect to zero-point energy and quasibound products.

proton transfer cross sections, the $v^+=0$ measurement was affected by secondary collisions that lowered the apparent threshold. The signal-to-noise was insufficient to conduct a proper zero-pressure extrapolation. Nevertheless, the cross sections above threshold are consistent with the earlier GIB measurements, and the deconvoluted results are in good agreement with the quantum scattering results. Note that in the latter case, significant errors may have been introduced in the digitization given the expanded vertical scale of the respective figures. Both corrected and uncorrected QCT cross sections are significantly lower than the deconvoluted cross sections near threshold.

The effect of secondary collisions is significantly smaller in the $v^+=1$ case, where the cross sections are substantially larger. The modified LOC model fit produces a threshold energy (Table I) that is within 0.01 eV of the expected thermal energy threshold of 0.512 eV. The present measurements are somewhat lower than the GIB work of Achtenhagen⁵⁹ above $E_T=1$ eV. This may be the result of impure state-selection when using a multiphoton ionization scheme. The comparison is poorer with the measurements of Turner *et al.*,⁵⁷ where the data exhibit a more gradual increase in cross section with energy throughout the displayed energy range. Meanwhile, somewhat surprisingly given the

relatively poor control of ion energy, the measurements of Chupka and co-workers,^{9,10} as presented by Kumar *et al.*,^{60,79} are in very satisfactory agreement with the present measurements.

The small curvature parameter, n , listed for $v^+=1$ in Table I is indicative of a sharp threshold. This is consistent with the quantum scattering results. While the time-dependent quantum mechanical study by Maiti *et al.*⁴⁵ using the MTJS surface is in very good agreement with the present results, the quantum scattering studies by Lepetit and Launay⁴¹ using the same surface, not shown in the figure, and those by Aquilanti *et al.*⁴⁸ on the Palmieri surface, predict significantly higher cross sections above $E_T=0.7$ eV. The comparison with the raw experimental data and the uncorrected QCT results is deceptively good. However, the finite cross section below the threshold for reaction demonstrates the weakness of QCT when zero-point energy is not taken into account. The zero-point corrected data are significantly lower than the experimental results near threshold. At higher energy, the corrected QCT results and the experimental values converge.

The present experimental cross sections for $v^+=2$ exceed 1 \AA^2 above threshold. The convoluted modified LOC model provides a good fit to the data near threshold, and the threshold energy of 0.248 eV (Table I) determined in a free fit of all three parameters is within 0.01 eV of the actual threshold (0.256 eV). Note that the fit is only applicable to near-threshold data, and that, therefore, the discrepancy at higher energies is of no significance.

The only experimental data that the present cross sections can be compared with are the two values of Turner *et al.* (closed squares)⁵⁷ and the two values reported by Chupka and co-workers (open diamonds).⁹ The latter results are within the experimental errors in good agreement with the present measurements. The uncorrected QCT results are slightly higher than the experimental results, while the zero-point corrected values exhibit a significantly less sharp onset at threshold. Above $E_T=1$ eV, the present experimental results agree nicely with both QCT sets. As for $v^+=1$, the quantum results exhibit a very sharp onset above which the cross sections exceed the present results by about a factor of 2.

The proton transfer reaction for reactants in $v^+=3$ is only endothermic by 0.038 eV, suggesting that the thermal rotational and translational energy are sufficient to drive the reaction. Nevertheless, the experimental data show clear threshold behavior. The LOC model fit produces a threshold of 0.082 eV, which is significantly higher than the actual threshold including thermal rotational energy of 0.015 eV. Since this threshold energy is significantly below the translational energy resolution of the present experiment near threshold, the inaccuracy of the deconvoluted threshold is not surprising. In fact, the derived threshold energy corresponds to about half the center-of-mass collision energy resolution (FWHM) at collision energies below 0.1 eV. The cross sections by Chupka *et al.*, as retrieved from their work,^{9,10} are in superb agreement with the present results. The measurements of Turner *et al.*⁵⁷ lie significantly below the present results. The present experimental measurements

TABLE II. PFI-PESICO and QCT cross sections determined for the respective product ion channels at a nominal translational energy of 0.6 eV. The QCT proton transfer cross sections correspond to channels with product vibrational energies exceeding the zero-point energy. QCT values both including and excluding quasibound collision product molecular ions are listed. Statistical errors are provided. Cross sections are given in \AA^2 .

v^+	PFI-PESICO	QCT/HeH ⁺	QCT/HeH ⁺ quasibound	QCT/H ⁺	QCT/H ⁺ quasibound
0					
1	0.626±0.105	0	0		
2	2.45±0.52	0.46±0.04	0.46±0.04		
3	4.83±0.24	1.57±0.10	1.57±0.10		
4	8.16±0.34	2.99±0.15	2.99±0.15		
5	7.60±0.73	3.79±0.18	3.79±0.18		
6	7.15±0.47	4.69±0.21	4.69±0.21		
7	7.46±0.51	5.52±0.22	5.52±0.22		
8	8.74±0.69	6.73±0.26	6.73±0.26		
9	6.95±0.70	7.12±0.26	7.12±0.26		
10	8.45±0.83	7.47±0.28	7.47±0.28		
11	9.10±0.98	8.30±0.29	8.44±0.29	0.744±0.097	0.487±0.079
12	7.98±0.73	7.64±0.31	8.00±0.32	3.34±0.22	2.72±0.20
13	5.08±0.53	5.62±0.28	6.08±0.29	6.36±0.30	5.73±0.28
14	5.83±0.33	4.50±0.25	4.76±0.25	9.21±0.33	8.74±0.33
15	4.42±0.39	2.98±0.25	3.11±0.25	12.87±0.47	12.60±0.46
16		2.51±0.23	2.60±0.23	16.22±0.51	15.71±0.50
17		1.61±0.16	1.62±0.16	19.21±0.43	18.92±0.43

are higher than the QCT results at low energies. At higher energies there is excellent agreement with the uncorrected QCT data, while experiment and corrected QCT results converge as the energy increases. Contrary to the $v^+=1$ and 2 cases, the quantum scattering results for $v^+=3$ are only slightly lower than the deconvoluted experimental results at the cross-section peak. At higher energies, the time-dependent results⁴⁵ are essentially identical to the present measurements.

B. PFI-PESICO measurements of $\text{H}_2^+(v^+, N^+=1)+\text{He}$ proton transfer cross sections at selected translational energies

PFI-PESICO measurements at translational energies, E_T , of 0.6 and 3.1 eV are shown in Fig. 3 as a function of reactant vibrational quantum number. The error bars reflect the statistical errors, which are considerably smaller than the estimated $\pm 40\%$ error in absolute experimental values. This estimate stems from the comparison between $v^+ < 4$ PFI-PESICO measurements and values obtained using the technique described in Sec. IV A. The experimental data are compared with zero-point corrected QCT proton transfer and collision-induced dissociation (CID) cross sections that are also corrected for quasibound products. The results are listed in Tables II and III, where the cross sections without quasibound corrections are included since they provide a more appropriate comparison to other theories. It is noted that the effect of quasibound states surviving for times comparable to our instrument flight times is not significant. At $E_T=0.6$ eV, the PFI-PESICO cross sections are significantly higher than the QCT cross sections at low v^+ . Above $v^+=3$, the PFI-PESICO cross sections reach a plateau of approximately 8\AA^2 before they decline due to competition with the dissociation channel that has an onset at $v^+=11$. In this energy

range, the agreement between QCT and experiment is very satisfactory. The present measurements are compared with state-selected relative cross sections recorded at $E_T=0.57$ eV by Koyano and co-workers.^{26,58} Their data were scaled through a least-squares fit to the present results.

At $E_T=3.1$ eV, the measured cross sections are in excellent agreement with the zero-point corrected QCT results for all measurements. The present experimental data are also compared with the experimental results of Govers and Guyon,⁸² who, using a threshold photoelectron coincidence approach, reported values for the largest range of vibrational states, $v^+=0-6$. The measurements of Govers and Guyon were not absolute and were scaled to the cross sections of Chupka. Given the experimental errors, the agreement between the present results and the reported values of Govers and Guyon is very good. The agreement with the least-squares scaled results of Koyano and co-workers^{26,58} is also very satisfactory. Interestingly, the nearly equal cross sections for $v^+=1$ and 2 observed by the latter agree with the observations of Govers and Guyon, but differ from the present experimental results as well as the QCT predictions.

C. Recoil velocities from PFI-PESICO measurements

The PFI-PESICO measurements comprise TOF measurements with respect to a PFI-electron trigger. The time-resolved proton-transfer ion intensity measurements thus provide information on the distribution of laboratory velocity components parallel to the flight axis, v'_{1p} . Figure 4 compares HeH⁺ TOF measurements inverted to velocity distributions, $f(v'_{1p})$, for $v^+=3$ and 4 at a collision energy of 0.6 eV. These vibrational states were picked since they represent the transition from endothermic to exothermic proton transfer, and because there is a significant difference between the PFI-

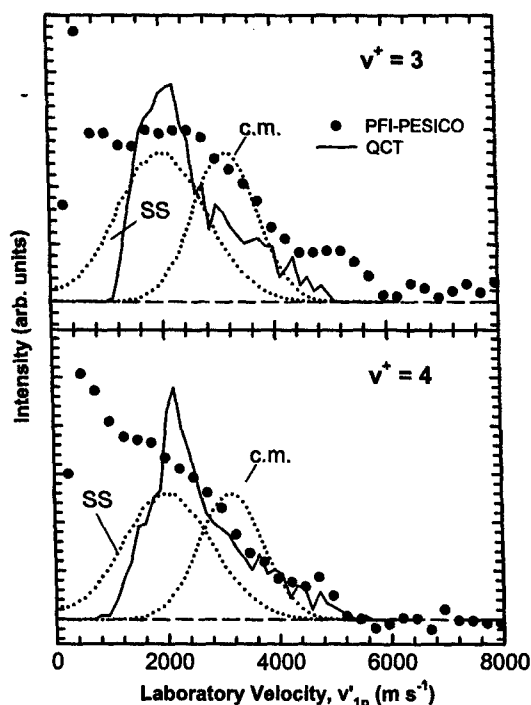


FIG. 4. Velocity-inverted PFI-PESICO TOF spectra of proton transfer product ions, HeH^+ (PFI-PESICO), formed at $E_T=0.6$ eV (c.m.) collision energy with reactant H_2^+ ions state-selected in $v^+=3$ and 4. The experimental results are compared with present QCT predictions. The latter have not been corrected with respect to zero-point energy and quasibound products. SS refers to velocity projections predicted for a spectator stripping mechanism, and "c.m." is the distribution of velocity projections for products formed at the c.m. velocity.

PESICO and QCT results at $E_T=0.6$ eV. The measurements are compared with distributions extracted from the QCT calculations for the same initial conditions. The dotted curves are simulations of the kinematically broadened c.m. laboratory velocity distribution, $f(v'_{\text{c.m.}})$, and a direct scattering event with energy transfer prescribed by the spectator stripping (SS) model.^{83,84} The SS translational-to-internal energy transfer at 0.6 eV is 0.36 eV.

Both the experimental and QCT distributions are backscattered with respect to the center-of-mass velocity, as ex-

pected in larger impact parameter events. The experimental maxima are close to zero laboratory velocities. At laboratory velocities below 1000 m s^{-1} , the present measurements become inaccurate due to TOF perturbations induced by surface potential barriers. Consequently, the experimental distributions are not fully conclusive as to where the maximum of the distribution is, since the low-velocity peak can be enhanced by obstructed ions. The $v^+=3$ experimental distribution is noticeably less strongly backscattered and exhibits a maximum close to the peak of the SS distribution and the QCT distribution. While the experimental distribution at $v^+=4$ appears to be more backscattered than at $v^+=3$, the QCT distribution is narrower and slightly less backscattered than the distribution at $v^+=3$ and the SS distribution. This does not signify inconsistency with a SS mechanism since angular scattering could shift the maximum toward higher laboratory velocity components. The comparison to QCT also must consider the fact that the distributions shown have not been corrected with respect to trajectories producing proton transfer products with vibrational energy below the zero-point energy.

V. DISCUSSION

This work provides the first beam measurements of state-selected integral reaction cross sections of the $\text{H}_2^+(v^+) + \text{He}$ proton transfer system for vibrational levels $v^+=7-15$. The $v^+=15$, $N^+=1$ level lies only 0.11 eV below the dissociation limit. Because an extensive body of theoretical work has focused on total energies below 2 eV, we have also remeasured the translational energy dependence of the proton-transfer cross section for $v^+=0-3$ at $E_T < 2$ eV (Fig. 2). Those measurements are in good agreement with the microscopic cross sections reported by Chupka^{9-11,60} for $v^+=0-3$ and GIB measurements by Achtenhagen *et al.*⁵⁹ for $v^+=0$ and 1. The agreement with the GIB measurements of Turner *et al.*⁵⁷ is less satisfactory. The low energy measurements are compared with QCT calculations performed on the most recent *ab initio* potential energy surface by Palmieri *et al.*⁴⁷ The experimental data appear to be well reproduced by the calculations that ignore zero-point energy effects. The zero-

TABLE III. PFI-PESICO and QCT cross sections determined for the respective product ion channels at a nominal translational energy of 3.1 eV. For explanations, see Table II.

v^+	PFI-PESICO	QCT/HeH ⁺	QCT/HeH ⁺ quasibound	QCT/H ⁺	QCT/H ⁺ quasibound
0	0.165±0.008	0.094±0.011	0.096±0.011	0.007±0.003	0.005±0.002
1	0.253±0.027	0.253±0.016	0.255±0.016	0.052±0.007	0.049±0.007
2	0.356±0.034	0.388±0.021	0.390±0.021	0.148±0.013	0.135±0.013
3	0.399±0.026	0.522±0.028	0.527±0.028	0.360±0.024	0.343±0.023
4	0.575±0.022	0.549±0.033	0.557±0.033	0.765±0.038	0.721±0.037
5	0.530±0.040	0.582±0.039	0.601±0.040	1.43±0.06	1.37±0.06
6	0.520±0.052	0.579±0.035	0.609±0.036	2.05±0.06	1.96±0.06
7	0.572±0.041	0.472±0.034	0.487±0.034	2.60±0.07	2.51±0.07
8	0.563±0.082	0.509±0.044	0.513±0.044	3.82±0.11	3.70±0.11
9	0.394±0.036	0.432±0.042	0.449±0.043	4.56±0.12	4.46±0.12
10	0.453±0.042	0.382±0.040	0.395±0.041	5.45±0.13	5.33±0.13
11	0.391±0.030	0.369±0.033	0.382±0.034	5.65±0.10	5.55±0.10
12	0.333±0.131	0.293±0.030	0.299±0.030	6.02±0.11	5.87±0.10

point energy corrected cross sections, on the other hand, are significantly lower than the measured cross sections near threshold. For all reactant states investigated in Fig. 2, the experimental measurements converge with the zero-point energy corrected cross sections as the collision energy increases.

A very similar observation has been made in the $\text{H}_2^+(v^+)+\text{Ne}$ system, where the discrepancy near threshold has been attributed to the effect of quantum scattering resonances.³ The importance of such resonances has been widely documented for the present system.^{14,15,30-38,85} 3D quantum scattering calculations of the integral reaction cross section using the MTJS^{41,45} and Palmieri⁴⁸ surfaces capture the near-threshold behavior better than the QCT calculations. The quantum calculations predict a very rapid increase of the proton transfer cross section at threshold, corresponding to curvature parameters [Eq. (3)], n , significantly less than 1. Such low curvature parameters are indicative of longer-lived intermediates.⁸¹ Near the cross-section maxima, the agreement between the quantum calculations and the present experiments is very satisfactory for reactants in $v^+=0$ and 3. For $v^+=1$ and 2, the theoretical cross sections at the highest collision energies investigated above threshold exceed the experimental cross sections substantially. The fact that the $v^+=2$ PFI-PESICO measurement at $E_T=0.6$ eV is significantly higher than the measurement at the same translational energy in Fig. 2 suggests that the autoionization approach taken in the latter measurement may have resulted in significant $v^+=0$ and 1 population. The satisfactory comparison with other beam experiments, however, would suggest that, if impure state selection is the source of the discrepancy, the other experiments are similarly affected. Nevertheless, the comparison with the quantum scattering studies is markedly improved in the present system compared with the H_2^++Ne system, where theory dramatically overpredicted proton transfer cross sections for $v^+=1$ and 2.³ Barring important shortcomings in the quantum scattering studies, this suggests that the potential energy surfaces derived for the H_2^++He system are of significantly higher quality than the H_2^++Ne surface provided by Pendergast and co-workers,⁸ and that the improved accuracy of the surface significantly affects the dynamics calculations.

The state-selected cross sections measured for $E_T=0.6$ eV (Fig. 3) are significantly higher than the zero-point corrected QCT values up to $v^+=5$, which corresponds to a total energy of ~ 2 eV. At higher vibrational levels, the agreement with the classical scattering results is very satisfactory. For H_2^++Ne , the agreement between experiment and QCT calculations was excellent at total energies between 1 and 3 eV.⁴⁰ The disagreement at higher total energies was attributed to either an inaccurate potential or nonadiabatic effects associated with the repulsive first excited electronic state of H_2^+ . In the present system, the PFI-PESICO cross sections for the highest v^+ states at $E_T=0.6$ eV as well as all of the measurements at $E_T=3.1$ eV are in excellent agreement with the QCT calculations. Both the PFI-PESICO measurements and the QCT calculations at 0.6 eV exhibit a sharp onset to the decline of the cross sections above $v^+=11$ due to the rapidly increasing CID cross section with v^+ . It is par-

ticularly encouraging that the $E_T=3.1$ eV measurements are in such good agreement given the fact that proton transfer competes with the dissociation channel for all reactant vibrational states at this translational energy.

The good agreement between QCT and experiment at energies where the CID cross section is significant suggests that nonadiabatic effects may not play an important role in the present proton transfer system, despite the smaller reduced mass in comparison with the H_2^++Ne system. This is consistent with conclusions made by Sizun and Gislason,²⁵ who conducted surface-hopping trajectory calculations using the Whitton-Kuntz DIM potentials.²⁰ At $E_T=3.1$ eV, they found that surface-hopping trajectories are not important in the proton-transfer channel. The proton transfer cross sections reported by Sizun and Gislason for $v^+=0, 3, 6,$ and 10 are in reasonable agreement with the present measurements and QCT results; the largest discrepancy is encountered for $v^+=0$. Approximately a third of the dissociation trajectories, however, were found to involve surface hopping. Except for $v^+=0$, where the present calculated dissociation cross section of 0.007 \AA^2 is significantly lower than their value of 0.047 \AA^2 , the dissociation cross sections calculated by Sizun and Gislason are within 25% of the present calculations that involve a single potential energy surface. We are currently in the process of measuring and calculating cross sections for the D_2^++He CID channel to further investigate the importance of nonadiabatic effects in dissociation collisions.

Despite the importance of resonances at low collision energies, the recoil velocity distributions for $v^+=3$ and 4 at $E_T=0.6$ eV (Fig. 4) suggest that the interaction is very direct resulting in primarily backscattered products. There is a hint of more momentum exchange in the $\text{H}_2^+(v^+=3, N^+=1)+\text{He}$ proton transfer reaction in comparison with the $\text{H}_2^+(v^+=4, N^+=1)+\text{He}$ reaction which is exothermic. Thus, the only manifestation of resonances in the present experiment is provided by the significant differences between the measured and QCT cross sections. The recoil velocity distributions are consistent with a spectator-stripping model,^{83,84} as previously pointed out by Herman and co-workers.^{58,62,64} In state-selected differential cross section measurements, Pollard *et al.*^{65,66} observed a clear shift toward more scattering at 0° c.m. angle versus 180° as the reactant vibrational state was raised from $v^+=0$ to 2 for collision energies ranging from 1.2 to 1.8 eV. The observed tendency toward more backscattering ($\sim 0^\circ$ c.m. scattering angle) was subtler at lower energies, where scattering was more skewed toward backscattering even for $v^+=0$ and 1. This is consistent with the present experimental and theoretical results and was interpreted as resulting from a larger percentage of low-impact parameter trajectories producing rebounding collisions at higher collision energies.

VI. CONCLUSIONS

New state-selected integral reaction cross sections determined with the guided-ion beam (GIB) technique in conjunction with high-resolution VUV reactant ion preparation and a PFI-PESICO approach are reported for the $\text{H}_2^+(v^+)+\text{He}$ proton transfer reaction. The translational energy dependence

measurements for $v^+ = 0-3$ are in good agreement with most previous experiments. The excellent signal-to-noise in the kinematically broadened experiments allowed a cross-section deconvolution based on the modified line-of-centers model.^{80,81} Threshold energies correspond within error to the thermodynamic limits except for $v^+ = 0$, where the low signal levels may be affected by secondary collisions. The deconvoluted results exhibit a sharp increase in cross section at threshold corresponding to low curvature parameters, n . This sharp increase is consistent with 3D quantum reactive scattering calculations of integral reaction cross sections.^{41,45,48}

At $E_T = 0.6$ eV, cross sections were measured for reactant states in $N^+ = 1$ and $v^+ = 1-15$. The comparison of the measured cross sections with QCT calculations taking zero-point energy effects into account is poor for $v^+ < 6$, suggesting important quantum effects. At higher reactant levels, the experimental and QCT cross sections agree within the experimental uncertainties. A decline in cross section above $v^+ = 11$ is attributed to competition with the CID channel. At $E_T = 3.1$ eV, excellent agreement between the present PFI-PESICO and QCT calculations is observed throughout the investigated range of vibrational quantum states, $v^+ = 0-12$. The remarkable agreement between the present measurements and QCT at high total energies suggests that nonadiabatic effects do not contribute significantly to the integral cross section. The present results also nicely validate the high accuracy of the potential energy surface by Palmieri *et al.*⁴⁷

ACKNOWLEDGMENTS

This work has been supported by AFOSR through task 2303EP02 and Grant No. F49620-99-1-0234 (Program Manager, Michael R. Berman). C.Y.N. also acknowledges support by the NSF Grant No. ATM-0001646 and partial support by the U. S. Department of Energy, Office of Basic Energy Sciences, Division of Chemical Sciences, Geosciences, and Biosciences. We thank D. De Fazio for sending us his code of the $H_2^+ + He$ potential. We also appreciate helpful comments by N. Sathyamurthy.

- ¹X. Qian, T. Zhang, Y. Chiu, D. J. Levandier, J. S. Miller, R. A. Dressler, and C. Y. Ng, *J. Chem. Phys.* **118**, 2455 (2003).
- ²X. Qian, T. Zhan, C. Chang, P. Wang, C. Y. Ng, Y. Chiu, D. J. Levandier, J. S. Miller, R. A. Dressler, T. Baer, and D. S. Peterka, *Rev. Sci. Instrum.* **74**, 4096 (2003).
- ³T. Zhang, X. M. Qian, X. N. Tang, C. Y. Ng, Y. Chiu, D. J. Levandier, J. S. Miller, and R. A. Dressler, *J. Chem. Phys.* **119**, 10175 (2003).
- ⁴J. Kress, R. B. Walker, E. F. Hayes, and P. Pendergast, *J. Chem. Phys.* **100**, 2728 (1994).
- ⁵M. Gilibert, X. Giménez, F. Huarte-Larrañaga, M. González, A. Aguilar, I. Last, and M. Baer, *J. Chem. Phys.* **110**, 6278 (1999).
- ⁶F. Huarte-Larrañaga, X. Giménez, J. M. Lucas, A. Aguilar, and J. M. Launay, *Phys. Chem. Chem. Phys.* **1**, 1125 (1999).
- ⁷F. Huarte-Larrañaga, X. Giménez, J. M. Lucas, A. Aguilar, and J. M. Launay, *J. Phys. Chem.* **104**, 10227 (2000).
- ⁸P. Pendergast, J. M. Heck, E. F. Hayes, and R. Jaquet, *J. Chem. Phys.* **98**, 4543 (1993).
- ⁹W. A. Chupka, J. Berkowitz, and M. E. Russell, in *Sixth International Conference on the Physics of Electronic and Atomic Collisions, Abstracts of Papers* (MIT, Cambridge, 1969), pp. 71-72.
- ¹⁰W. A. Chupka, in *Ion-molecule Reactions*, edited by J. L. Franklin (Plenum, New York, 1972), Vol. 1.
- ¹¹W. A. Chupka and M. E. Russell, *J. Chem. Phys.* **49**, 5426 (1968).

- ¹²C. Stroud, N. Sathyamurthy, R. Rangarajan, and L. M. Raff, *Chem. Phys. Lett.* **48**, 350 (1977).
- ¹³N. Sathyamurthy, R. Rangarajan, and L. M. Raff, *J. Chem. Phys.* **64**, 4606 (1976).
- ¹⁴D. J. Kouri and M. Baer, *Chem. Phys. Lett.* **24**, 37 (1974).
- ¹⁵J. T. Adams, *Chem. Phys. Lett.* **33**, 275 (1975).
- ¹⁶N. Balakrishnan and N. Sathyamurthy, *Comput. Phys. Commun.* **63**, 209 (1991).
- ¹⁷N. Sathyamurthy, *Chem. Phys. Lett.* **59**, 95 (1978).
- ¹⁸N. Sathyamurthy, *Chem. Phys.* **62**, 1 (1981).
- ¹⁹P. J. Kuntz and W. N. Whitton, *Chem. Phys. Lett.* **34**, 340 (1975).
- ²⁰W. N. Whitton and P. J. Kuntz, *J. Chem. Phys.* **64**, 3624 (1976).
- ²¹P. J. Kuntz, *Chem. Phys. Lett.* **16**, 581 (1972).
- ²²P. J. Brown and E. F. Hayes, *J. Chem. Phys.* **55**, 922 (1971).
- ²³N. Sathyamurthy and L. M. Raff, *J. Chem. Phys.* **63**, 464 (1975).
- ²⁴C. Zuhrt, F. Schneider, U. Havemann, L. Züllicke, and Z. Herman, *Chem. Phys.* **38**, 205 (1979).
- ²⁵M. Sizon and E. A. Gislason, *J. Chem. Phys.* **91**, 4603 (1989).
- ²⁶M. Baer, S. Suzuki, K. Tanaka, I. Koyano, H. Nakamura, Z. Herman, and D. J. Kouri, *Phys. Rev. A* **34**, 1748 (1986).
- ²⁷T. Joseph and N. Sathyamurthy, *J. Chem. Phys.* **80**, 5332 (1987).
- ²⁸T. Joseph and N. Sathyamurthy, *J. Chem. Phys.* **86**, 704 (1987).
- ²⁹D. R. McLaughlin and D. L. Thompson, *J. Chem. Phys.* **70**, 2748 (1979).
- ³⁰F. M. Chapman and E. F. Hayes, *J. Chem. Phys.* **62**, 4400 (1975).
- ³¹F. M. Chapman and E. F. Hayes, *J. Chem. Phys.* **65**, 1032 (1976).
- ³²T. Joseph and N. Sathyamurthy, *J. Indian Chem. Soc.* **62**, 874 (1985).
- ³³N. Sathyamurthy, M. Baer, and T. Joseph, *Chem. Phys.* **114**, 73 (1987).
- ³⁴N. Balakrishnan and N. Sathyamurthy, *Chem. Phys. Lett.* **201**, 294 (1993).
- ³⁵N. Balakrishnan and N. Sathyamurthy, *Chem. Phys. Lett.* **240**, 119 (1995).
- ³⁶K. Sakimoto and K. Onda, *Chem. Phys. Lett.* **226**, 227 (1994).
- ³⁷S. Mahapatra and N. Sathyamurthy, *J. Chem. Phys.* **102**, 6057 (1995).
- ³⁸S. Mahapatra and N. Sathyamurthy, *J. Chem. Phys.* **105**, 10934 (1996).
- ³⁹J. D. Kress, R. B. Walker, and E. F. Hayes, *J. Chem. Phys.* **93**, 8085 (1990).
- ⁴⁰J. Z. H. Zhang, D. L. Yeager, and W. H. Miller, *Chem. Phys. Lett.* **173**, 489 (1990).
- ⁴¹B. Lepetit and J. M. Launay, *J. Chem. Phys.* **95**, 51595168 (1991).
- ⁴²S. Mahapatra and N. Sathyamurthy, *J. Chem. Phys.* **107**, 6621 (1997).
- ⁴³C. Kalyanaraman, D. C. Clary, and N. Sathyamurthy, *J. Chem. Phys.* **111**, 10910 (1999).
- ⁴⁴B. Maiti, S. Mahapatra, and N. Sathyamurthy, *J. Chem. Phys.* **113**, 59 (2000).
- ⁴⁵B. Maiti, C. Kalyanaraman, A. Panda, and N. Sathyamurthy, *J. Chem. Phys.* **117**, 9719 (2002).
- ⁴⁶A. Aguado and M. Paniagua, *J. Chem. Phys.* **96**, 1265 (1992).
- ⁴⁷P. Palmieri, C. Puzzarini, V. Aquilanti, G. Capecchi, S. Cavalli, D. De Fazio, A. Aguilar, X. Gimenez, and J. M. Lucas, *Mol. Phys.* **98**, 1839 (2000).
- ⁴⁸V. Aquilanti, G. Capecchi, S. Cavalli, D. De Fazio, P. Palmieri, C. Puzzarini, A. Aguilar, X. Gimenez, and J. M. Lucas, *Chem. Phys. Lett.* **318**, 619 (2000).
- ⁴⁹J. M. Hutson and A. Ernesti, *Mol. Phys.* **96**, 457 (1999).
- ⁵⁰M. Meuwly and J. M. Hutson, *J. Chem. Phys.* **110**, 3418 (1999).
- ⁵¹S. Kumar, H. Kapoor, and N. Sathyamurthy, *J. Chem. Phys.* **103**, 6021 (1998).
- ⁵²K. R. Ryan and I. G. Graham, *J. Chem. Phys.* **59**, 4260 (1973).
- ⁵³R. D. Smith, D. L. Smith, and J. H. Futrell, *Int. J. Mass Spectrom. Ion Phys.* **19**, 369 (1976).
- ⁵⁴D. von Pijkeren, E. Boltjes, J. von Eck, and A. Niehaus, *Chem. Phys.* **91**, 293 (1984).
- ⁵⁵D. von Pijkeren, J. von Eck, and A. Niehaus, *Chem. Phys. Lett.* **96**, 20 (1983).
- ⁵⁶J. C. Light, *J. Chem. Phys.* **41**, 586587 (1964).
- ⁵⁷T. Turner, O. Dutoit, and Y. T. Lee, *J. Chem. Phys.* **81**, 3475 (1984).
- ⁵⁸Z. Herman and I. Koyano, *J. Chem. Soc., Faraday Trans. 2* **83**, 127 (1987).
- ⁵⁹M. Achtenhagen, M. Schweizer, and D. Gerlich, private communication reported by S. Kumar, N. Sathyamurthy, and K. C. Balla, *J. Chem. Phys.* **98**, 4680 (1993).
- ⁶⁰S. Kumar, N. Sathyamurthy, and K. C. Balla, *J. Chem. Phys.* **98**, 4680 (1993).
- ⁶¹S. L. Anderson, *Adv. Chem. Phys.* **82**, 177 (1992).

- ⁶²F. Schneider, U. Havemann, L. Zülicke, V. Pacak, K. Birkinshaw, and Z. Herman, *Chem. Phys. Lett.* **37**, 323 (1976).
- ⁶³U. Havemann, V. Pacak, Z. Herman, F. Schneider, C. Zuhrt, and L. Zülicke, *Chem. Phys.* **28**, 147 (1978).
- ⁶⁴V. Pacak, U. Havemann, Z. Herman, F. Schneider, and L. Zülicke, *Chem. Phys. Lett.* **49**, 273 (1977).
- ⁶⁵J. E. Pollard, L. K. Johnson, and R. B. Cohen, *J. Chem. Phys.* **95**, 4894 (1991).
- ⁶⁶J. E. Pollard, L. K. Johnson, and R. B. Cohen, *J. Chem. Phys.* **94**, 8615 (1991).
- ⁶⁷K. C. Bhalla and N. Sathyamurthy, *Chem. Phys. Lett.* **160**, 437 (1989).
- ⁶⁸G. K. Jarvis, Y. Song, and C. Y. Ng, *Rev. Sci. Instrum.* **70**, 2615 (1999).
- ⁶⁹G. K. Jarvis, K.-M. Weitzel, M. Malow, Y. Song, and C. Y. Ng, *Rev. Sci. Instrum.* **70**, 3892 (1999).
- ⁷⁰N. E. Bradbury and R. A. Nielsen, *Phys. Rev.* **49**, 388 (1936).
- ⁷¹P. R. Vlasak, D. J. Beussman, M. R. Davenport, and C. G. Enke, *Rev. Sci. Instrum.* **67**, 68 (1996).
- ⁷²N. R. Daly, *Rev. Sci. Instrum.* **31**, 264 (1960).
- ⁷³P. M. Dehmer and W. A. Chupka, *J. Chem. Phys.* **65**, 2243 (1976).
- ⁷⁴M. A. O'Halloran, P. M. Dehmer, F. S. Tomkins, S. T. Pratt, and J. L. Dehmer, *J. Chem. Phys.* **89**, 75 (1988).
- ⁷⁵P. J. Chantry, *J. Chem. Phys.* **55**, 2746 (1971).
- ⁷⁶R. A. Dressler and E. Murad, in *Unimolecular and Bimolecular Ion-Molecule Reaction Dynamics*, edited by C. Y. Ng, T. Baer, and I. Powis (Wiley, New York, 1994).
- ⁷⁷S. Chapman, D. L. Bunker, and A. Gelb, Program No. 273 Quantum Chemical Program Exchange, 1974.
- ⁷⁸P. J. Kuntz, in *Atom-Molecule Collision Theory*, edited by R. B. Bernstein (Plenum, New York, 1979).
- ⁷⁹S. Kumar, H. Kapoor, and N. Sathyamurthy, *Chem. Phys. Lett.* **289**, 361 (1998).
- ⁸⁰C. Rebick and R. D. Levine, *J. Chem. Phys.* **58**, 3942 (1973).
- ⁸¹R. D. Levine and R. B. Bernstein, *J. Chem. Phys.* **56**, 2281 (1972).
- ⁸²T. R. Govers and P.-M. Guyon, *Chem. Phys.* **113**, 425 (1987).
- ⁸³A. Henglein, in *Ion-Molecule Reactions in the Gas Phase*, edited by P. J. Ausloos (American Chemical Society, Washington, DC, 1966), Vol. 58, p. 63.
- ⁸⁴A. Henglein and K. Lacmann, *Adv. Mass Spectrom.* **3**, 331 (1966).
- ⁸⁵S. Mahapatra, R. Ramaswamy, and N. Sathyamurthy, *J. Chem. Phys.* **104**, 3989 (1996).